Code equations

Yvonne Ban

30 July 2019

Contents

1 Empirical inputs **4**

2 Constants **4**
2.1 VI, volume of inductor 4
2.2 nsq, number of squares of inductor 5
2.3 nu_opt, frequency of photons 5
2.4 E_gamma, energy of photons 5
2.5 delta0, gap energy at 0K 5
2.6 delta, gap energy at T 6
2.7 sigma_n, normal conductivity just above Tc 6
2.8 lambL, (London) penetration depth in the thin film limit 6
2.9 N0, single-spin density of electron states at Fermi energy 7
2.10 N_qp_photon, number of quasiparticles produced per photon 7

3 Intrinsic parameters (intrinsic to material) **7**
3.1 R_qp, intrinsic quasiparticle recombination constant 7

4 Thermal parameters (depend on T) **8**
4.1 n_qp_therm, quasiparticle density due to thermal effects at T 8
4.2 gamma_G, low-temperature thermal generation rate at T 8

5 Steady-state parameters **8**
5.1 tau_phon_es, phonon escape time 8
5.2 F_phon, phonon trapping factor 9
5.3 R_eff, effective quasiparticle recombination constant 9
5.4 tau_qp, quasiparticle relaxation time 10
5.5 n_qp_ss, steady-state quasiparticle density 10
5.6 N_qp_ss, steady-state quasiparticle number in resonator 10

6 Optical generation **11**
6.1 gamma_opt, constant optical power quasiparticle generation rate 11

7 All together now 11
7.1 N_qp_tot, total number of quasiparticles in resonator due to thermal and constant optical power effects . . . 11

8 Complex conductivity 12
8.1 sigma1_0, real part of complex conductivity at T=0K . . . 12
8.2 sigma2_0, imag part of complex conductivity at T=0K . . . 12
8.3 sigma1rat, ratio of real part of complex conductivity to quasiparticle density response at T . . . 12
8.4 sigma2rat, ratio of imag part of complex conductivity to quasiparticle density response at T . . . 13
8.5 sigma1, real part of complex conductivity at T . . . 13
8.6 sigma2, imag part of complex conductivity at T . . . 13
8.7 sigma, complex conductivity at T . . . 14

9 Surface impedance, reactance, (kinetic) inductance, resistance 14
9.1 Zs_0, surface impedance in thin film local limit at T=0K . . . 14
9.2 Zs, surface impedance in thin film local limit at T . . . 15
9.3 Xs_0, surface reactance in thin film local limit at T=0K . . . 15
9.4 Xs, surface reactance in thin film local limit at T . . . 15
9.5 Rs, surface resistance in thin film local limit at T . . . 16
9.6 Lk_0, kinetic inductance in thin film local limit at T=0K . . . 16
9.7 Lk, kinetic inductance in thin film local limit at T . . . 16

10 Resonant frequency 17
10.1 alpha, effective kinetic inductance fraction in thin film local limit . . . 17
10.2 f0, resonant frequency of resonator circuit at T=0K . . . 17
10.3 ffrac, fractional frequency shift in resonant frequency of circuit . . . 18
10.4 fnew, resonant frequency of resonator circuit in thin film local limit . . . 18
10.5 fdet, detuning of resonant frequency from readout frequency . . . 18

11 Quality factors 19
11.1 Q_qp, quality factor of resonator circuit from quasiparticles . . . 19
11.2 Qr, quality factor of resonator circuit in thin film local limit . . . 19

12 Responsivities 20
12.1 dPabs_dPinc, responsivity of absorbed optical power to incident optical power 20
12.2 dGamma_dP, responsivity of quasiparticle generation rate to optical power . 20
12.3 dN_qp_tot_dGamma, responsivity of N_qp_tot to quasiparticle generation rate 20
12.4 dsig1_dN, responsivity of sigma1 to N_qp_tot . . . 21
12.5 dsig2_dN, responsivity of sigma2 to N_qp_tot . . . 21
12.6 dRs_dsig1, responsivity of surface resistance Rs to sigma1 . . . 22
12.7 dXs_dsig2, responsivity of surface reactance Xs to sigma2 . . . 22
12.8 dlambqp_dRs, responsivity of quasiparticle loss factor lambda_qp to surface resistance Rs . . . 23

12.9 dx_dXs, responsivity of frequency detuning x to surface reactance Xs 23
12.10 dQqp_dRs, responsivity of quasiparticle quality factor Q_qp to surface resistance Rs 24

13 S21 **24**
13.1 S21, resonator quality factor of resonator circuit in thin film local limit . . . 24

14 NEP **24**
14.1 nep_phot, noise equivalent power (NEP) of photon noise 24
14.2 nep_rec, noise equivalent power (NEP) of recombination noise due to P_opt . 25

15 Finding P_opt **25**
15.1 P_opt_r, P_opt value from fnew 25

16 What doesn't work yet **26**
16.1 f0 resonance frequency 26
16.2 ffrac too low 26
16.3 Qr too low or drops too quickly 28
16.4 Singularity in L_k 28

1 Empirical inputs

Input	Value	Confidence
wI, width of inductor	4×10^{-6} m	100%
lI, length of inductor	4×10^{-4} m	100%
tI, thickness of inductor	1.8×10^{-8} m	100%
Tc, critical temperature	1.4 K	100%
tau0, characteristic electron-phonon interaction time	4.38×10^{-7} s	0%
T, operating temperature	0.1 K	100%
R_nsp, normal sheet resistivity	90 Ohms/square	100%
lamb, wavelength of photons	1.1×10^{-3} m	100%
delta_nuopt, optical bandwidth	1×10^{10} Hz	90%
Lg, geometric inductance	3×10^{-9} H	100%
C, capacitor capacitance in circuit	5×10^{-12} F	100%
eta_opt, optical efficiency	0.8	100%
eta_pb, pair-breaking efficiency	0.57	100%
tau_phon_br, time for phonon to break Cooper pair	1×10^{-10} s	0%
Qc, coupling quality factor	5×10^{4}	100%
nqp0, quasiparticle density at 0K	1×10^{20} m^{-3}	100%
P_read, readout power	6.31×10^{-12} W	0%
T_amp, amplifier noise temperature	3 K	0%
deltav_read, readout bandwidth	50 Hz	0%
V_read, readout voltage	1.776×10^{-5} V	0%

Table 1: Empirical inputs

2 Constants

2.1 VI, volume of inductor

Input	Confidence
wI, width of inductor	100%
lI, length of inductor	100%
tI, thickness of inductor	100%

Table 2: Inputs to VI, volume of inductor

$$V_I = w_I l_I t_I$$

2.2 nsq, number of squares of inductor

Input	Confidence
wI, width of inductor	100%
lI, length of inductor	100%

Table 3: Inputs to nsq, number of squares of inductor

$$n_{\mathrm{sq}} = \frac{w_I}{l_I}$$

2.3 nu_opt, frequency of photons

Input	Confidence
lamb, wavelength of photons	100%

Table 4: Inputs to nu_opt, frequency of photons

$$\nu_{\mathrm{opt}} = c\lambda$$

2.4 E_gamma, energy of photons

Input	Confidence
nu_opt, frequency of photons	100%

Table 5: Inputs to E_gamma, energy of photons

$$E_\gamma = h\nu_{\mathrm{opt}}$$

2.5 delta0, gap energy at 0K

Flanigan p.20 and Jay

Input	Confidence
Tc, critical temperature	100%

Table 6: Inputs to delta0, gap energy at 0K

$$\Delta_0 = 1.764kT_c$$

2.6 delta, gap energy at T

Zmuidzinas eq.4, basically identical to delta0.

Input	Confidence
delta0, gap energy at 0K	100%

Table 7: Inputs to delta, gap energy at T

$$\Delta = \Delta_0 \left(1 - \sqrt{2\pi k \Delta_0} e^{\frac{\Delta_0}{kT}}\right)$$

2.7 sigma_n, normal conductivity just above Tc

Flanigan (private correspondence)

Input	Confidence
R_nsp, normal sheet resistivity	100%
tI, thickness of inductor	100%

Table 8: Inputs to sigma_n, normal conductivity just above Tc

$$\sigma_n = \frac{1}{R_{\mathrm{nsq}} t_I}$$

2.8 lambL, (London) penetration depth in the thin film limit

Zmuidzinas eq.12 (currently unused)

Input	Confidence
sigma_n, normal conductivity just above Tc	50%
tI, thickness of inductor	100%

Table 9: Inputs to lambL, (London) penetration depth in the thin film limit

$$\lambda_L = \frac{\hbar}{\pi \mu_0 t_I \Delta \sigma_n}$$

2.9 N0, single-spin density of electron states at Fermi energy

Flanigan eq.3.10

Input	Confidence
T, operating temperature	100%
delta0, gap energy at 0K	100%

Table 10: Inputs to N0, single-spin density of electron states at Fermi energy

$$N_0 = \frac{n_{\mathrm{qp},0}}{2\sqrt{2\pi kT\Delta_0}e^{-\frac{\Delta_0}{kT}}}$$

2.10 N_qp_photon, number of quasiparticles produced per photon

Flanigan eq.3.67

Input	Confidence
eta_pb, pair-breaking efficiency	100%
nu_opt, frequency of photons	100%
delta, gap energy at T	100%

Table 11: Inputs to N_qp_photon, number of quasiparticles produced per photon

$$N_{\mathrm{qp,phot}} = \frac{h\eta_{\mathrm{pb}}\nu_{\mathrm{opt}}}{\Delta}$$

3 Intrinsic parameters (intrinsic to material)

3.1 R_qp, intrinsic quasiparticle recombination constant

Flanigan eq.3.14

Input	Confidence
delta0, gap energy at 0K	100%
N0, single-spin density of electron states at Fermi energy	90%
tau0, characteristic electron-phonon interaction time	0%

Table 12: Inputs to R_qp, intrinsic quasiparticle recombination constant

$$R_{\text{qp}} = \frac{2\left(\frac{\Delta_0}{kT_c}\right)^3}{N_0 \Delta_0 \tau_0}$$

4 Thermal parameters (depend on T)

4.1 n_qp_therm, quasiparticle density due to thermal effects at T

Flanigan eq.3.10

Input	Confidence
delta0, gap energy at 0K	100%
N0, single-spin density of electron states at Fermi energy	90%
T, operating temperature	100%

Table 13: Inputs to n_qp_therm, quasiparticle density due to thermal effects at T

$$n_{\text{qp,therm}} = 2N_0\sqrt{2\pi kT\Delta_0}e^{-\frac{\Delta_0}{kT}}$$

4.2 gamma_G, low-temperature thermal generation rate at T

Flanigan eq.3.17

Input	Confidence
delta0, gap energy at 0K	100%
N0, single-spin density of electron states at Fermi energy	90%
tau0, characteristic electron-phonon interaction time	0%
T, operating temperature	100%
Tc, critical temperature	100%

Table 14: Inputs to gamma_G, low-temperature thermal generation rate at T

$$\gamma_G = \frac{16N_0\Delta_0^3\pi T}{\tau_0 k^2 T_c^3}e^{-\frac{2\Delta_0}{kT}}$$

5 Steady-state parameters

5.1 tau_phon_es, phonon escape time

Flanigan eq.3.19 (currently unused)

Input	Confidence
tI, thickness of inductor	100%
eta_phon_trans, transmission probability per encounter	0%
s, probably speed of sound	0%

Table 15: Inputs to tau_phon_es, phonon escape time

$$\tau_{\text{phon,es}} = \frac{4t_I}{s\eta_{\text{phon, es}}}$$
$$\eta_{\text{phon,es}} = 1 \times 10^{-9}$$
$$s = 6.4 \times 10^3\,\text{ms}^{-1}$$

5.2 F_phon, phonon trapping factor

Flanigan eq.3.20 (currently unused)

Input	Confidence
tau_phon_br, time for phonon to break Cooper pair	0%
tau_phon_es, phonon escape time	0%

Table 16: Inputs to F_phon, phonon trapping factor

$$F_{\text{phon}} = 1 + \frac{\tau_{\text{phon,es}}}{\tau_{\text{phon,br}}}$$

5.3 R_eff, effective quasiparticle recombination constant

Flanigan p.31 (currently ignores F_phon)

Input	Confidence
R_qp, intrinsic quasiparticle recombination constant	0%
F_phon, phonon trapping factor	0%

Table 17: Inputs to R_eff, effective quasiparticle recombination constant

$$R_{\text{eff}} = \frac{R_{\text{qp}}}{F_{\text{phon}}}$$

5.4 tau_qp, quasiparticle relaxation time

Flanigan p.46 (currently unused)

Input	Confidence
R_eff, effective quasiparticle recombination constant	0%
gamma_G, low-temperature thermal generation rate at T	0%

Table 18: Inputs to tau_qp, quasiparticle relaxation time

$$\tau_{\mathrm{qp}} = \frac{1}{\sqrt{4 R_{\mathrm{eff}} \gamma_G}}$$

5.5 n_qp_ss, steady-state quasiparticle density

Flanigan p.43. Should match nqp0, assuming ignoring F_phon. tau0 term cancels out from R_eff and gamma_G.

Input	Confidence
R_eff, effective quasiparticle recombination constant	0%
gamma_G, low-temperature thermal generation rate at T	0%

Table 19: Inputs to n_qp_ss, steady-state quasiparticle density

$$n_{\mathrm{qp,ss}} = \sqrt{\frac{\gamma_G}{R_{\mathrm{eff}}}}$$

5.6 N_qp_ss, steady-state quasiparticle number in resonator

Flanigan p.57. tau0 term cancels out from R_eff and gamma_G.

Input	Confidence
R_eff, effective quasiparticle recombination constant	0%
gamma_G, low-temperature thermal generation rate at T	0%
VI, volume of inductor	100%

Table 20: Inputs to N_qp_ss, steady-state quasiparticle number in resonator

$$N_{\mathrm{qp,ss}} = V_I \sqrt{\frac{\gamma_G}{R_{\mathrm{eff}}}}$$

6 Optical generation

6.1 gamma_opt, constant optical power quasiparticle generation rate

Flanigan eq.3.68

Input	Confidence
P_opt, incident optical power	100%
dGamma_dP, responsivity of quasiparticle generation rate to optical power	100%
eta_pb, pair-breaking efficiency	100%
delta, gap energy at T	100%

Table 21: Inputs to gamma_opt, constant optical power quasiparticle generation rate

$$\gamma_{\mathrm{opt}} = \frac{dP_{\mathrm{abs}}}{dP_{\mathrm{inc}}} \frac{P_{\mathrm{opt}} \eta_{\mathrm{pb}}}{\Delta}$$

7 All together now

7.1 N_qp_tot, total number of quasiparticles in resonator due to thermal and constant optical power effects

Flanigan p.57. tau0 term cancels out between R_eff and gamma_G, but not between R_eff and gamma_opt. Effects are transmitted forward to fnew and Q_qp.

Input	Confidence
P_opt, incident optical power	100%
gamma_opt, constant optical power quasiparticle generation rate	100%
R_eff, effective quasiparticle recombination constant	0%
gamma_G, low-temperature thermal generation rate at T	0%
VI, volume of inductor	100%

Table 22: Inputs to N_qp_tot, total number of quasiparticles in resonator due to thermal and constant optical power effects

$$N_{\mathrm{qp,tot}} = V_I \sqrt{\frac{\gamma_G + \gamma_{\mathrm{opt}}(P_{\mathrm{opt}})}{R_{\mathrm{eff}}}}$$

8 Complex conductivity

8.1 sigma1_0, real part of complex conductivity at T=0K

Flanigan p.35

Input	Confidence

Table 23: Inputs to sigma1_0, real part of complex conductivity at T=0K

$$\sigma_1(0) = 0$$

8.2 sigma2_0, imag part of complex conductivity at T=0K

Flanigan p.35

Input	Confidence
sigma_n, normal conductivity just above Tc	100%
delta0, gap energy at 0K	100%
f, readout frequency	100%

Table 24: Inputs to sigma2_0, imag part of complex conductivity at T=0K

$$\sigma_2(0) = \frac{\pi \Delta_0 \sigma_n}{hf}$$

8.3 sigma1rat, ratio of real part of complex conductivity to quasiparticle density response at T

Flanigan eq.3.79. Used in dsig1_dN.

Input	Confidence
delta0, gap energy at 0K	100%
f, readout frequency	100%
T, operating temperature	100%

Table 25: Inputs to sigma1rat, ratio of real part of complex conductivity to quasiparticle density response at T

$$\Upsilon_{\sigma_1}(f) = \sqrt{\frac{8\Delta_0}{\pi^3 kT}} \sinh \frac{hf}{2kT} K_0 \left(\frac{hf}{2kT} \right)$$

8.4 sigma2rat, ratio of imag part of complex conductivity to quasiparticle density response at T

Flanigan eq.3.80. Used in dsig2_dN.

Input	Confidence
delta0, gap energy at 0K	100%
f, readout frequency	100%
T, operating temperature	100%

Table 26: Inputs to sigma2rat, ratio of imag part of complex conductivity to quasiparticle density response at T

$$\Upsilon_{\sigma_2}(f) = -1 - \sqrt{\frac{2\Delta_0}{\pi kT}} e^{-\frac{hf}{2kT}} I_0\left(\frac{hf}{2kT}\right)$$

8.5 sigma1, real part of complex conductivity at T

Uses dsig1_dN.

Input	Confidence
P_opt, incident optical power	100%
N_qp_tot, total number of quasiparticles in resonator	90%
sigma1_0, real part of complex conductivity at T=0K	100%
dsig1_dN, responsivity of sigma1 against N_qp_tot	100%
f, readout frequency	100%

Table 27: Inputs to sigma1, real part of complex conductivity at T

$$\sigma_1(f) = N_{\mathrm{qp,tot}}(P_{\mathrm{opt}}) \frac{d\sigma_1(f)}{dN_{\mathrm{qp}}} + \sigma_1(0)$$

8.6 sigma2, imag part of complex conductivity at T

Uses dsig2_dN.

Input	Confidence
P_opt, incident optical power	100%
N_qp_tot, total number of quasiparticles in resonator	90%
sigma2_0, imag part of complex conductivity at T=0K	100%
dsig2_dN, responsivity of sigma2 against N_qp_tot	100%
f, readout frequency	100%

Table 28: Inputs to sigma2, imag part of complex conductivity at T

$$\sigma_2(f) = N_{\mathrm{qp,tot}}(P_{\mathrm{opt}})\frac{d\sigma_2(f)}{dN_{\mathrm{qp}}} + \sigma_2(f, 0)$$

8.7 sigma, complex conductivity at T

Flanigan p.34

Input	Confidence
P_opt, incident optical power	100%
sigma1, real part of complex conductivity at T	90%
sigma2, imag part of complex conductivity at T	90%
f, readout frequency	100%

Table 29: Inputs to sigma, complex conductivity at T

$$\sigma(f) = \sigma_1(f, P_{\mathrm{opt}}) - i\sigma_2(f, P_{\mathrm{opt}})$$

9 Surface impedance, reactance, (kinetic) inductance, resistance

9.1 Zs_0, surface impedance in thin film local limit at T=0K

Flanigan eq.3.35

Input	Confidence
sigma2_0, imag part of complex conductivity at T=0K	100%
tI, thickness of inductor	100%
f, readout frequency	100%

Table 30: Inputs to Zs_0, surface impedance in thin film local limit at T=0K

$$Z_s(f,0) = \frac{i}{t_I \sigma_2(f,0)}$$

9.2 Zs, surface impedance in thin film local limit at T

Flanigan eq.3.35

Input	Confidence
P_opt, incident optical power	100%
sigma, complex conductivity at T	90%
tI, thickness of inductor	100%
f, readout frequency	100%

Table 31: Inputs to Zs, surface impedance in thin film local limit at T

$$Z_s(f) = \frac{1}{t_I \sigma(f, P_{\rm opt})}$$

9.3 Xs_0, surface reactance in thin film local limit at T=0K

Flanigan p.36

Input	Confidence
Zs_0, surface impedance in thin film local limit at T=0K	100%
f, readout frequency	100%

Table 32: Inputs to Xs_0, surface reactance in thin film local limit at T=0K

$$X_s(f,0) = \Im(Z_s(f,0))$$

9.4 Xs, surface reactance in thin film local limit at T

Flanigan p.36

Input	Confidence
P_opt, incident optical power	100%
Zs, surface impedance in thin film local limit at T	90%
f, readout frequency	100%

Table 33: Inputs to Xs, surface reactance in thin film local limit at T

$$X_s(f) = \Im(Z_s(f, P_{\text{opt}}))$$

9.5 Rs, surface resistance in thin film local limit at T

Flanigan p.36

Input	Confidence
P_opt, incident optical power	100%
Zs, surface impedance in thin film local limit at T	90%
f, readout frequency	100%

Table 34: Inputs to Rs, surface resistance in thin film local limit at T

$$R_s(f) = \Re(Z_s(f, P_{\text{opt}}))$$

9.6 Lk_0, kinetic inductance in thin film local limit at T=0K

Flanigan p.36

Input	Confidence
nsq, number of squares of inductor	100%
tI, thickness of inductor	100%
delta0, gap energy at 0K	100%
sigma_n, normal conductivity just above Tc	100%

Table 35: Inputs to Lk_0, kinetic inductance in thin film local limit at T=0K

$$L_k(0) = \frac{n_{\text{sq}} h}{2\pi^2 t_I \Delta_0 \sigma_n}$$

9.7 Lk, kinetic inductance in thin film local limit at T

Flanigan p.36

Input	Confidence
P_opt, incident optical power	100%
tI, thickness of inductor	100%
delta0, gap energy at 0K	100%
sigma_n, normal conductivity just above Tc	100%
N0, single-spin density of electron states at Fermi energy	90%
VI, volume of inductor	100%
sigma2rat, ratio of real part of complex conductivity to quasiparticle density response at T	100%

Table 36: Inputs to Lk, kinetic inductance in thin film local limit at T

$$L_k = L_k(0)\left(1 - \frac{N_{\text{qp,tot}}(P_{\text{opt}})\Upsilon_{\sigma_2}(f)}{2N_0\Delta_0 V_I + N_{\text{qp,tot}}(P_{\text{opt}})\Upsilon_{\sigma_2}(f)}\right)$$

10 Resonant frequency

10.1 alpha, effective kinetic inductance fraction in thin film local limit

Flanigan eq.3.62

Input	Confidence
Lk_0, kinetic inductance in thin film local limit at T=0K	100%
Lg, geometric inductance	100%

Table 37: Inputs to alpha, effective kinetic inductance fraction in thin film local limit

$$\alpha = \frac{L_k(0)}{L_g + L_k(0)}$$

10.2 f0, resonant frequency of resonator circuit at T=0K

Flanigan p.52

Input	Confidence
Lk_0, kinetic inductance in thin film local limit at T=0K	100%
Lg, geometric inductance	100%
C, capacitor capacitance in circuit	100%

Table 38: Inputs to f0, resonant frequency of resonator circuit at T=0K

$$f_0 = \frac{1}{2\pi\sqrt{C(L_g + L_k(0))}}$$

10.3 ffrac, fractional frequency shift in resonant frequency of circuit

Flanigan eq.3.63

Input	Confidence
alpha, effective kinetic inductance fraction in thin film local limit	100%
P_opt, incident optical power	100%
Lk, kinetic inductance in thin film local limit at T	90%
Lk_0, kinetic inductance in thin film local limit at T=0K	100%

Table 39: Inputs to ffrac, fractional frequency shift in resonant frequency of circuit

$$s = \frac{\alpha}{2}\frac{L_k(f, P_{\text{opt}}) - L_k(0)}{L_k(0)}$$

10.4 fnew, resonant frequency of resonator circuit in thin film local limit

Flanigan eq.3.61

Input	Confidence
P_opt, incident optical power	100%
f0, resonant frequency of resonator circuit at T=0K	100%
ffrac, fractional frequency shift in resonant frequency of circuit	90%

Table 40: Inputs to fnew, resonant frequency of resonator circuit in thin film local limit

$$f_{\text{new}} = f_0(1 - s(f, P_{\text{opt}}))$$

10.5 fdet, detuning of resonant frequency from readout frequency

Flanigan p.50

Input	Confidence
P_opt, incident optical power	100%
f, readout frequency	100%
fnew, resonant frequency of resonator circuit in thin film local limit	90%

Table 41: Inputs to fdet, detuning of resonant frequency from readout frequency

$$x = \frac{f}{f_{\mathrm{new}}(f, P_{\mathrm{opt}})} - 1$$

11 Quality factors

11.1 Q_qp, quality factor of resonator circuit from quasiparticles

Flanigan eq.3.64

Input	Confidence
alpha, effective kinetic inductance fraction in thin film local limit	100%
P_opt, incident optical power	100%
Xs_0, surface reactance in thin film local limit at T=0K	100%
Rs, surface resistance in thin film local limit at T	90%
f, readout frequency	100%

Table 42: Inputs to Q_qp, quality factor of resonator circuit from quasiparticles

$$Q_{\mathrm{qp}}(f) = \frac{X_s(f, 0)}{\alpha R_s(f, P_{\mathrm{opt}})}$$

11.2 Qr, quality factor of resonator circuit in thin film local limit

Flanigan eq.3.58. Assumes internal quality factor Q_i is dominated by Q_qp.

Input	Confidence
P_opt, incident optical power	100%
Q_qp, quality factor of resonator circuit from quasiparticles	90%
Qc, coupling quality factor	100%
f, readout frequency	100%

Table 43: Inputs to Qr, quality factor of resonator circuit in thin film local limit

$$Q_{\mathrm{r}} = \left(\frac{1}{Q_c} + \frac{1}{Q_{\mathrm{qp}}(f, P_{\mathrm{opt}})} \right)^{-1}$$

12 Responsivities

12.1 dPabs_dPinc, responsivity of absorbed optical power to incident optical power

Flanigan eq.3.66

Input	Confidence
eta_opt, optical efficiency	100%

Table 44: Inputs to dPabs_dPinc, responsivity of absorbed optical power to incident optical power

$$\frac{dP_{\mathrm{abs}}}{dP_{\mathrm{inc}}} = \eta_{\mathrm{opt}}$$

12.2 dGamma_dP, responsivity of quasiparticle generation rate to optical power

Flanigan eq.3.69

Input	Confidence
eta_pb, pair-breaking efficiency	100%
delta0, gap energy at 0K	100%

Table 45: Inputs to dGamma_dP, responsivity of quasiparticle generation rate to optical power

$$\frac{d\gamma_{\mathrm{opt}}}{dP_{\mathrm{opt}}} = \frac{\eta_{\mathrm{pb}}}{\Delta_0}$$

12.3 dN_qp_tot_dGamma, responsivity of N_qp_tot to quasiparticle generation rate

Flanigan eq.3.72

Input	Confidence
P_opt, incident optical power	100%
gamma_opt, constant optical power quasiparticle generation rate	100%
R_eff, effective quasiparticle recombination constant	0%
gamma_G, low-temperature thermal generation rate at T	0%
VI, volume of inductor	100%

Table 46: Inputs to dN_qp_tot_dGamma, responsivity of N_qp_tot to quasiparticle generation rate

$$\frac{dN_{\text{qp,tot}}}{d\gamma} = \frac{1}{2}\sqrt{\frac{V_I}{R_{\text{eff}}(\gamma_G + \gamma_{\text{opt}}(P_{\text{opt}}))}}$$

12.4 dsig1_dN, responsivity of sigma1 to N_qp_tot

Flanigan eq.3.81. Uses sigma1rat and used in calculation of sigma1.

Input	Confidence
sigma2_0, imag part of complex conductivity at T=0K	100%
sigma1rat, ratio of real part of complex conductivity to quasiparticle density response at T	100%
N0, single-spin density of electron states at Fermi energy	100%
delta0, gap energy at 0K	100%
VI, volume of inductor	100%
f, readout frequency	100%

Table 47: Inputs to dsig1_dN, responsivity of sigma1 to N_qp_tot

$$\frac{d\sigma_1(f)}{dN_{\text{qp,tot}}} = \frac{\sigma_2(f,0)\Upsilon_{\sigma_1}(f)}{2N_0\Delta_0 V_I}$$

12.5 dsig2_dN, responsivity of sigma2 to N_qp_tot

Flanigan eq.3.82. Uses sigma2rat and used in calculation of sigma2.

Input	Confidence
sigma2_0, imag part of complex conductivity at T=0K	100%
sigma2rat, ratio of real part of complex conductivity to quasiparticle density response at T	100%
N0, single-spin density of electron states at Fermi energy	100%
delta0, gap energy at 0K	100%
VI, volume of inductor	100%
f, readout frequency	100%

Table 48: Inputs to dsig2_dN, responsivity of sigma2 to N_qp_tot

$$\frac{d\sigma_2(f)}{dN_{\text{qp,tot}}} = \frac{\sigma_2(f,0)\Upsilon_{\sigma_2}(f)}{2N_0\Delta_0 V_I}$$

12.6 dRs_dsig1, responsivity of surface resistance Rs to sigma1

Flanigan eq.3.83

Input	Confidence
Xs_0, surface reactance in thin film local limit at T=0K	100%
sigma2_0, imag part of complex conductivity at T=0K	100%
f, readout frequency	100%

Table 49: Inputs to dRs_dsig1, responsivity of surface resistance Rs to sigma1

$$\frac{dR_s(f)}{d\sigma_1} = \frac{X_s(f,0)}{\sigma_2(f,0)}$$

12.7 dXs_dsig2, responsivity of surface reactance Xs to sigma2

Flanigan eq.3.84

Input	Confidence
Xs_0, surface reactance in thin film local limit at T=0K	100%
sigma2_0, imag part of complex conductivity at T=0K	100%
f, readout frequency	100%

Table 50: Inputs to dXs_dsig2, responsivity of surface reactance Xs to sigma2

$$\frac{dX_s(f)}{d\sigma_2} = -\frac{X_s(f,0)}{\sigma_2(f,0)}$$

12.8 dlambqp_dRs, responsivity of quasiparticle loss factor lambda_qp to surface resistance Rs

Flanigan eq.3.87

Input	Confidence
alpha, effective kinetic inductance fraction in thin film local limit	100%
P_opt, incident optical power	100%
Xs_0, surface reactance in thin film local limit at T=0K	100%
f, readout frequency	100%

Table 51: Inputs to dlambqp_dRs, responsivity of quasiparticle loss factor lambda_qp to surface resistance Rs

$$\frac{d\lambda_{\mathrm{qp}}}{dR_s(f)} = \frac{\alpha(P_{\mathrm{opt}})}{X_s(f,0)}$$

12.9 dx_dXs, responsivity of frequency detuning x to surface reactance Xs

Flanigan eq.3.88

Input	Confidence
alpha, effective kinetic inductance fraction in thin film local limit	100%
P_opt, incident optical power	100%
Xs_0, surface reactance in thin film local limit at T=0K	100%
f, readout frequency	100%

Table 52: Inputs to dx_dXs, responsivity of frequency detuning x to surface reactance Xs

$$\frac{dx}{dX_s(f)} = \frac{\alpha(P_{\mathrm{opt}})}{2X_s(f,0)}$$

12.10 dQqp_dRs, responsivity of quasiparticle quality factor Q_qp to surface resistance Rs

Input	Confidence
alpha, effective kinetic inductance fraction in thin film local limit	100%
P_opt, incident optical power	100%
Q_qp, quality factor of resonator circuit from quasiparticles	100%
Xs_0, surface reactance in thin film local limit at T=0K	100%
f, readout frequency	100%

Table 53: Inputs to dQqp_dRs, responsivity of quasiparticle quality factor Q_qp to surface resistance Rs

$$\frac{dQ_{\mathrm{qp}}(f)}{dR_s(f)} = -\frac{Q_{\mathrm{qp}}(f)^2\alpha(P_{\mathrm{opt}})}{X_s(f,0)}$$

13 S21

13.1 S21, resonator quality factor of resonator circuit in thin film local limit

Flanigan eq.3.60

Input	Confidence
P_opt, incident optical power	100%
f, readout frequency	100%
Q_r, quality factor of resonator circuit in thin film local limit	90%
Qc, coupling quality factor	100%
fdet, detuning of resonant frequency from readout frequency	90%
A, symmetry factor	90%

Table 54: Inputs to S21, resonator quality factor of resonator circuit in thin film local limit

$$S_{21} = 1 - \frac{Q_r(f,P_{\mathrm{opt}})(1+iA)}{Q_c(1+2iQ_r(f,P_{\mathrm{opt}})x(f,P_{\mathrm{opt}}))}$$

14 NEP

14.1 nep_phot, noise equivalent power (NEP) of photon noise

Flanigan eq.5.5, from shot noise and wave noise

Input	Confidence
P_opt, incident optical power	100%
nu_opt, frequency of photons	100%
delta_nuopt, optical bandwidth	90%

Table 55: Inputs to nep_phot, noise equivalent power (NEP) of photon noise

$$\mathrm{NEP}(P_{\mathrm{opt}}) = \sqrt{2\left(h\nu P_{\mathrm{opt}} + \frac{P_{\mathrm{opt}}^2}{\Delta\nu}\right)}$$

14.2 nep_rec, noise equivalent power (NEP) of recombination noise due to P_opt

Flanigan eq.5.19

Input	Confidence
P_opt, incident optical power	100%
delta0, gap energy at 0K	100%
eta_opt, optical efficiency	100%
eta_pb, pair-breaking efficiency	100%

Table 56: Inputs to nep_rec, noise equivalent power (NEP) of recombination noise due to P_opt

$$\mathrm{NEP}(P_{\mathrm{opt}}) = 2\sqrt{\frac{\Delta_0 P_{\mathrm{opt}}}{\eta_{\mathrm{opt}}\eta_{\mathrm{pb}}}}$$

15 Finding P_opt

15.1 P_opt_r, P_opt value from fnew

Input	Confidence
fnew, resonant frequency of resonator circuit	100%

Table 57: Inputs to P_opt_r, P_opt value from fnew

$$L_k(P_{\mathrm{opt}}) = 2(L_g + L_k(T=0))(1 - 2\pi f_{\mathrm{new}}\sqrt{C(L_g + L_k(T=0))}) + L_g$$
$$N_{\mathrm{qp,tot}} = -\frac{2N_0\Delta_0 V_I}{\Upsilon_{\sigma_2}(f)}\left(1 + \frac{L_k(T=0)}{L_k(P_{\mathrm{opt}})}\right)$$
$$P_{\mathrm{opt}} = \frac{\Delta}{\eta_{\mathrm{pb}}\eta_{\mathrm{opt}}}\left(\frac{N_{\mathrm{qp,tot}}^2 R_{\mathrm{eff}}}{V_I} - \gamma_G\right)$$

16 What doesn't work yet

16.1 f0 resonance frequency

With parameters meant to have fnew(0)=500 MHz, i.e. nqp0=10^{20} and R_nsq=90 Ω, and tau0 set at value for Al (4.38×10^{-7} s), actual fnew(0)=1.281 GHz. Linked to R_nsq.

16.2 ffrac too low

Fig. 1: With parameters set to have fnew(0)=500 kHz, i.e. nqp0=10^{20} and R_nsq=1.7536×10^4 Ω, and tau0 set at value for Al (4.38×10^{-7} s), ffrac changes very little with P_opt. Linked to nqp0.

Fig. 2 and Fig. 3: With only change from default being tau0=10 s, ffrac follows empirical trend.

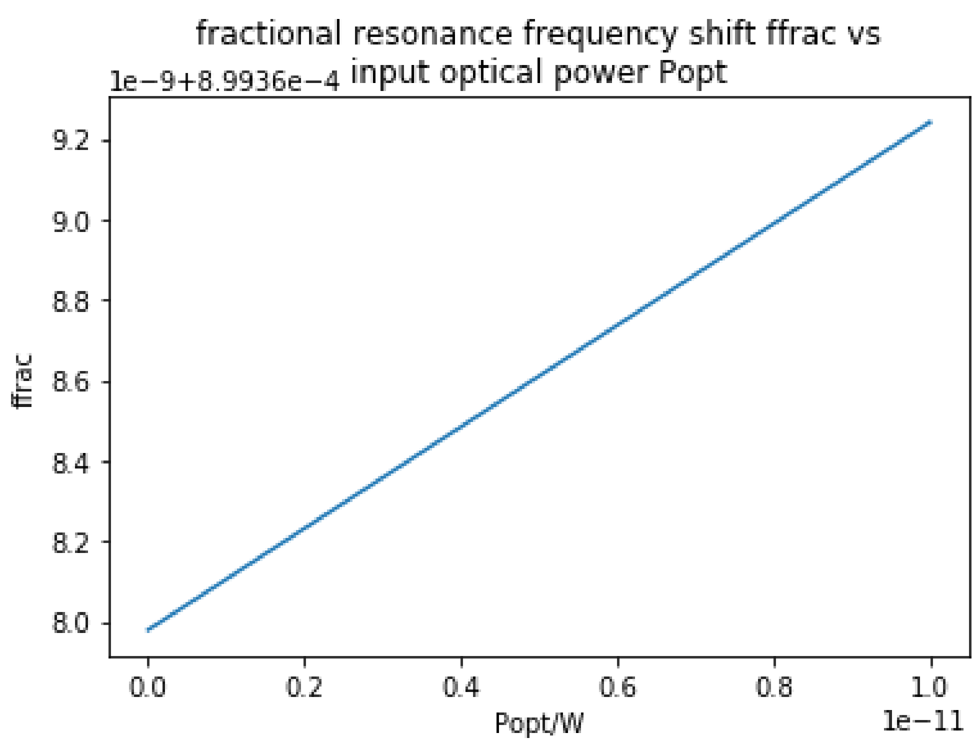

Figure 1: Fractional frequency shift with R_nsq=1.7536×10^4 Ω so fnew(0)=500 kHz.

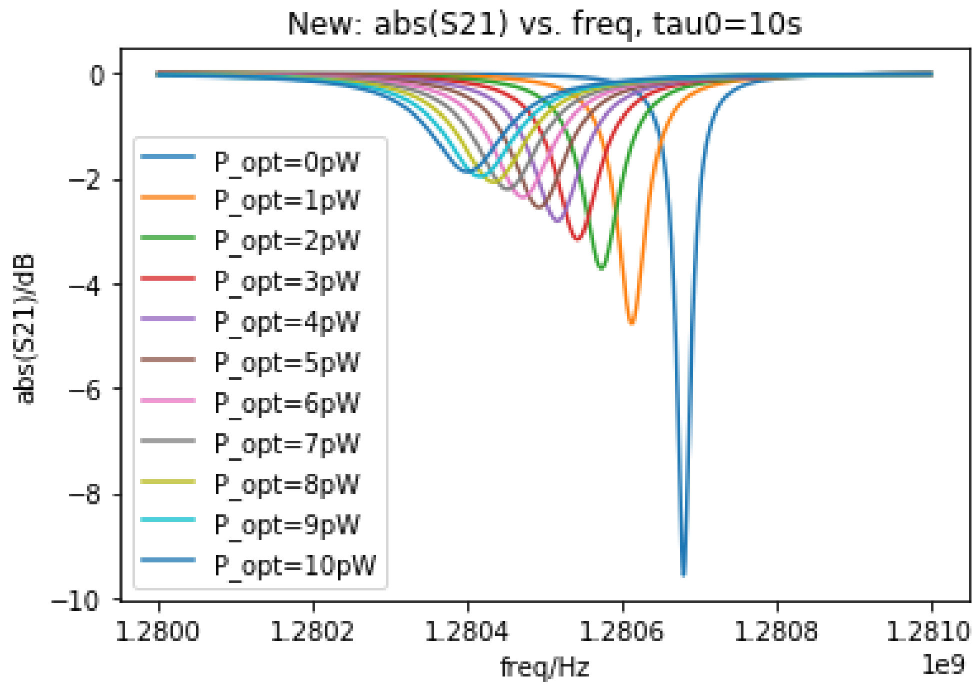

Figure 2: Resonance curves with only tau0 changed from 4.38×10^{-7} s to 10 s.

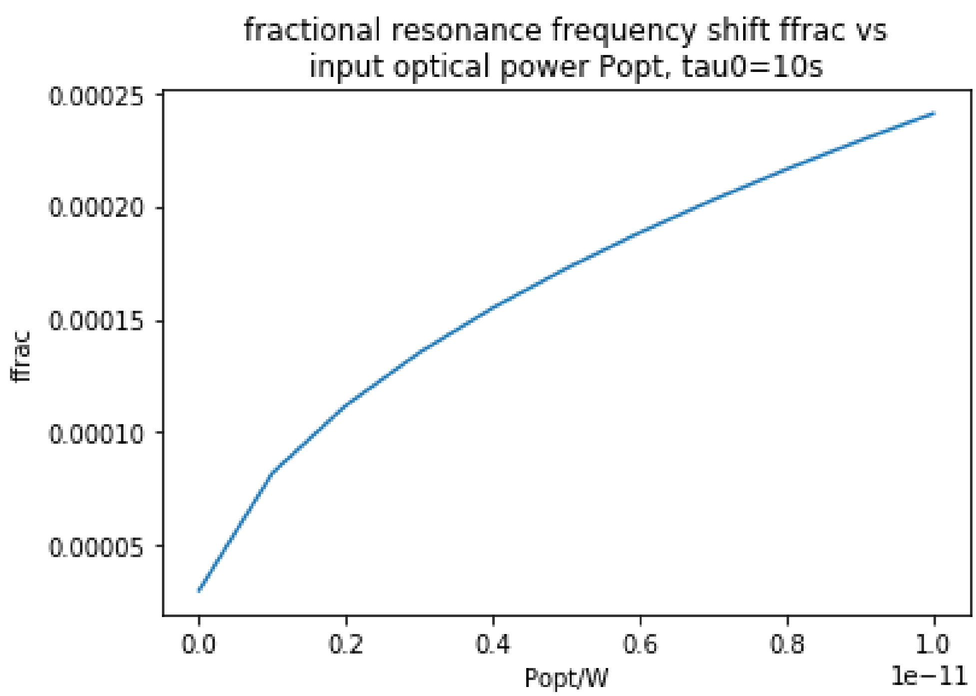

Figure 3: Fractional frequency shift with only tau0 changed from 4.38×10^{-7} s to 10 s.

16.3 Qr too low or drops too quickly

Fig. 4: With parameters set to have fnew(0)=500 kHz and tau0 set at value for Al (4.38×10^{-7} s), Qr too low or drops too quickly with P_opt. Linked to nqp0.

Fig. 5: With only change from default being tau0=10 s, Qr follows empirical trend.

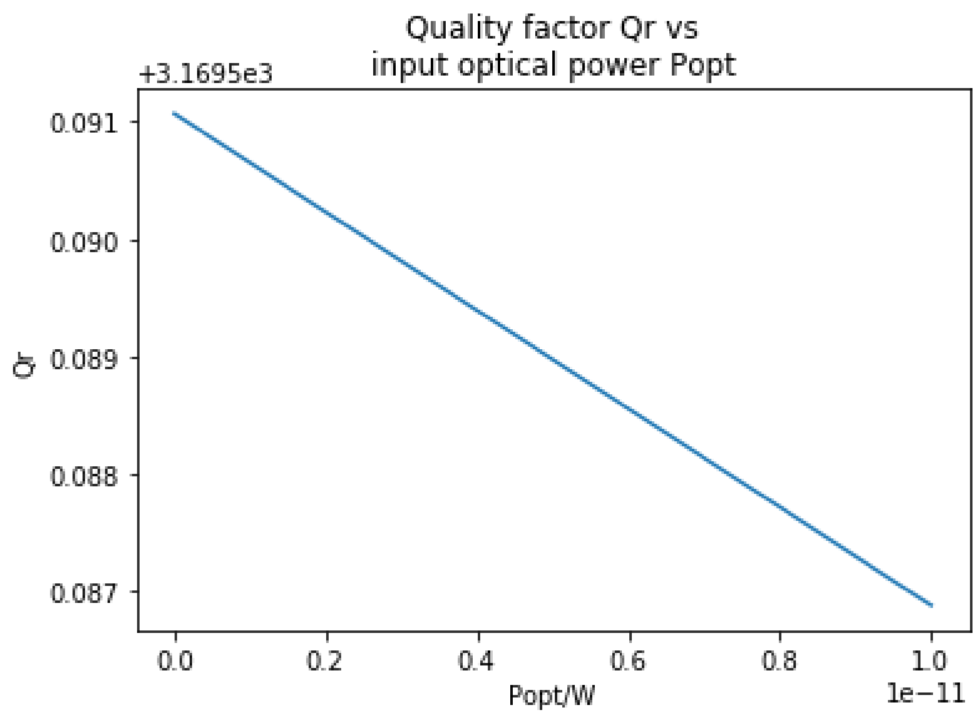

Figure 4: Quality factor with R_nsq=$1.7536 \times 10^4\,\Omega$ so fnew(0)=500 kHz.

16.4 Singularity in L_k

There is a singularity in L_k as a function of temperature T that affects resonance frequency fnew as shown in Fig. 6. It can be traced to the L_k denominator term $(2N_0\Delta_0 V_I + N_{\mathrm{qp,tot}}(P_{\mathrm{opt}})\Upsilon_{\sigma_2})$. The term sigma2rat, Υ_{σ_2}, is negative, while the other terms are positive. At the same time, N0 varies with temperature as shown in Fig. 7. This causes a zero to appear in the denominator for a certain value of T, causing the resonance frequency to blow up, which is obviously not physical.

HOWEVER, the calculation for sigma2rat (and sigma1rat) seems to be incorrect and is being reviewed. It may itself be dependent on frequency, which makes its use to calculate resonance frequency circular and problematic.

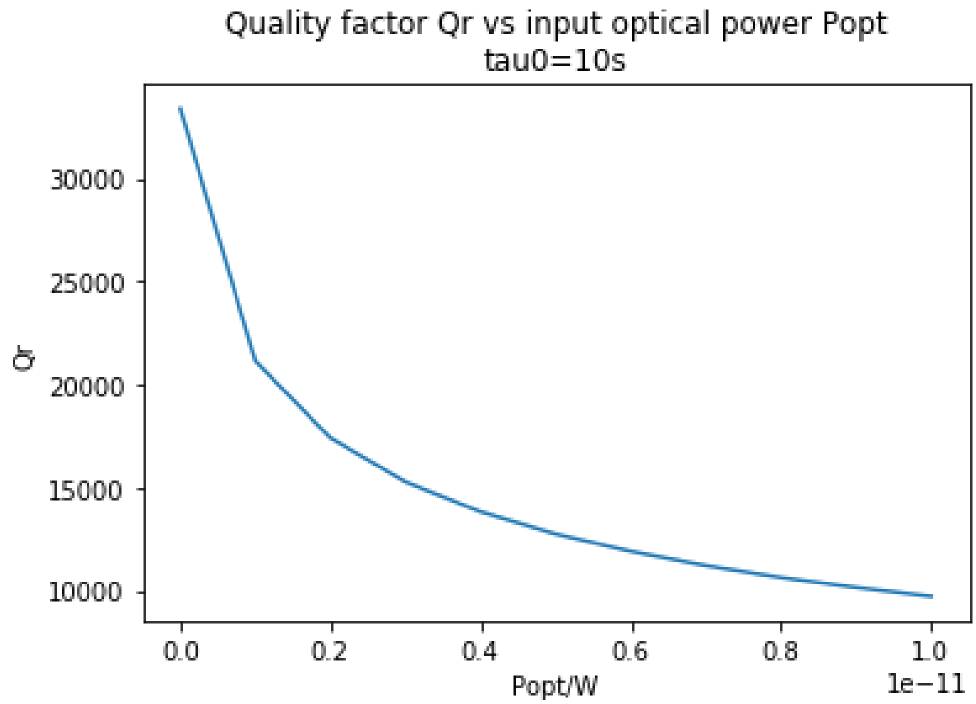

Figure 5: Quality factor with only tau0 changed from 4.38×10^{-7} s to 10 s.

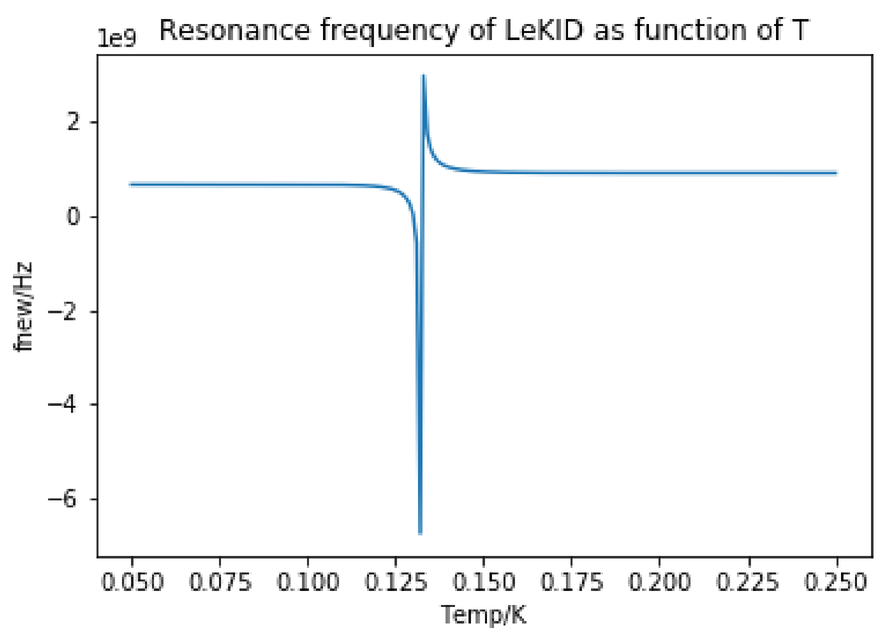

Figure 6: Singularity in resonance frequency as a function of temperature.

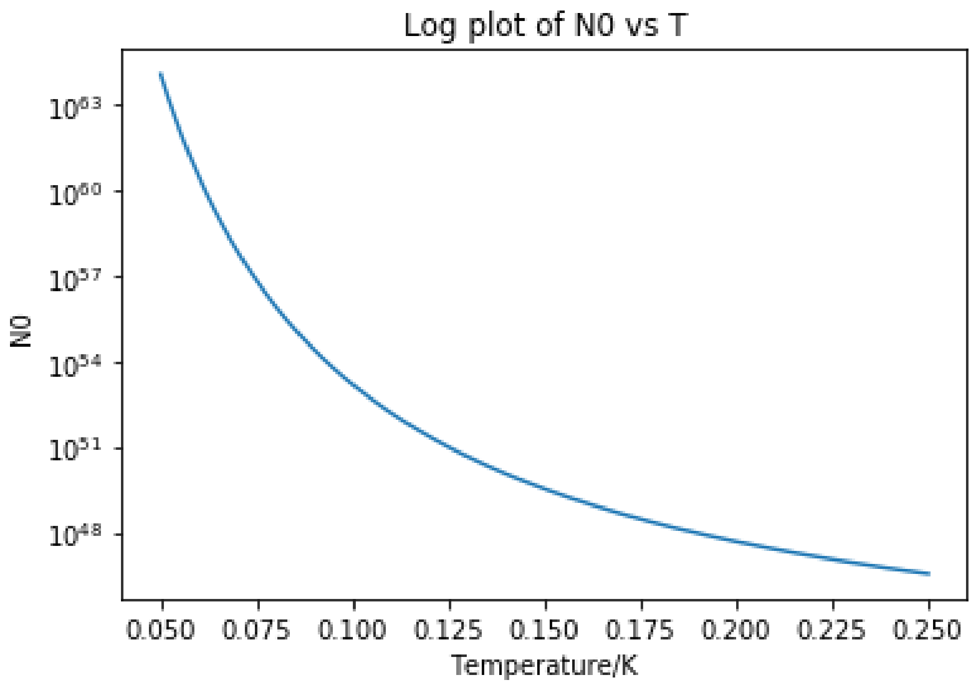

Figure 7: N0 as a function of temperature.